CONDENSATION HEAT TRANFER OF NON-AZEOTROPIC MIXTURES INSIDE CHANNELS

Azzolin M., Berto A., Bortolin S. and Del Col D.*
*Author for correspondence
Department of Industrial Engineering,
University of Padova, Padova, Italy
E-mail: davide.delcol@unipd.it

ABSTRACT

Binary or ternary blends of hydroflourocarbons (HFCs) and hydrofluoroolefins (HFOs) are recently emerging as possible substitutes for the high GWP (Global Warming Potential) fluids currently employed in refrigeration and air-conditioning industry. In the present paper, heat transfer coefficients of a ternary mixture of R1234yf, R32 and CO_2, ASHRAE designation R455A, 75.5/21.5/3.0 by mass composition, have been measured during condensation inside a minichannel having a 0.96 mm internal diameter and in a conventional tube with 8.0 mm diameter. Tests have been performed at 40°C mean saturation temperature. The present experimental database is used to assess available predicting correlations for condensation of mixtures, providing information on the applicability of available models.

INTRODUCTION

Starting from Montreal and Kyoto protocols, increasing attention has been paid to environmental protection and global warming. In Europe, the Regulation EU No 517/2014 foresees the introduction of a HFCs phase-down in the next years. The most affected refrigerants by the aforementioned regulation are R404A ($GWP_{100-years}$=3922), R410A ($GWP_{100-years}$=2088) and R134a ($GWP_{100-years}$=1430). Two pure halogenated olefins R1234yf ($GWP_{100-years}$=4) and R1234ze(E) ($GWP_{100-years}$<1) have been proposed for R134a replacement respectively in automotive air-conditioning and refrigeration systems. Currently, no pure fluids are available as alternatives to R410A in chiller and air-conditioning applications and to R404A in commercial and transport refrigeration that are able to meet the requirements in terms of system performance, low GWP and non-flammability. For these applications one possible solution can rely on refrigerant mixtures of HFOs and other HFCs (i.e. R32, R125). One of the characteristics of this non-azeotropic mixture is the variable temperature during phase change at constant pressure, due to the temperature glide between the dew and the bubble point. This phenomenon can lead to a better matching between the refrigerant and the water temperature profiles in a condenser. On the other hand, the additional mass transfer resistance which occurs during the phase change of zeotropic mixtures causes a heat transfer degradation; for this reason, it is fundamental to have reliable models for the correct design of heat exchangers.

In the literature, few studies are available on HFOs/HFCs mixtures and most of them are focused on the vaporization process. Hossain et al. [1] investigated the flow boiling heat transfer characteristics of the mixture R1234ze(E)/R32 at 55/45% mass fraction in horizontal tube with inner diameter of 4.35 mm, comparing them with those of R410A and R32 at the same operating conditions. The conclusions indicate that the local heat transfer coefficient is lower than that of R32 and R410A in the whole vapor quality region. With regard to R1234ze(E), the heat transfer coefficient of the zeotropic blend is lower only in the high quality region. Kondou et al. [2] investigated the condensation and evaporation heat transfer coefficients of mixtures R744/R32/R1234ze(E) and R32/R1234ze(E) at variable compositions in a horizontal microfin tube of 5.35 mm inner diameter. The authors found that both condensation and evaporation heat transfer coefficients of the mixtures are penalized with respect to single components and they tried to quantify the contribution of the additional mass transfer resistance. Wang et al. [3] experimentally studied the condensation heat transfer characteristics of R1234yf/R32 mixtures (mass fraction 52/48% and 77/23%) in a horizontal smooth tube of 4 mm inner diameter. They developed a prediction model for the forced convective condensation of zeotropic mixtures.

The aim of this work is to investigate the heat transfer performance of a zeotropic mixture when condensing inside smooth tubes with different diameters. The studied mixture is a ternary blend of R32, R1234yf and CO_2 (21.5/75.5/3.0 by mass composition) named R455A (ASHRAE designation) or L40X (commercial designation by Honeywell). This mildly flammable mixture ($GWP_{100-years}$=145) has been designed to serve as an alternative to R404A and R410A in commercial and transport refrigeration, in chillers and air-conditioning systems.

NOMENCLATURE

A	[m^2]	Exchange surface area
c_p	[J kg^{-1} K^{-1}]	Specific heat
d_i	[m]	Hydraulic diameter
e_{AB}	[-]	Absolute deviation
G	[kg m^{-2} s^{-1}]	Mass velocity
h	[J kg^{-1}]	Specific enthalpy
$\dot{m}$	[kg s^{-1}]	Mass flow rate
p	[Pa]	Pressure
q	[W]	Heat flow rate
q'	[W m^{-2}]	Heat flux
T	[K]	Temperature
x	[-]	Thermodynamic vapour quality
X	[-]	Mass fraction
z	[m]	Position
Special characters		
α	[W m^{-2} K^{-1}]	Heat transfer coefficient

| Δh	[J kg^{-1}]	Specific enthalpy difference		
ΔT	[K]	Temperature difference		
λ	[W m^{-1} K^{-1}]	Thermal conductivity		
μ	[μPa s]	Dynamic viscosity		
ρ	[kg m^{-3}]	Density		
Subscripts				
cond	Condensation		*mix*	Mixture
evap	Evaporation		*MS*	Measuring section
f	Film		*ref*	Refrigerant
g	Vapor		*s*	Sensible
GL	Glide		*sat*	Saturation
in	Inlet		*t*	Total
l	Liquid		*w*	Wall
LMTD	Logarithmic mean temperature difference			

EXPERIMENTAL FACILITIES AND HEAT TRANSFER TEST SECTIONS

The experimental tests have been conducted with two different test sections: one with inner diameter of 8.0 mm and the other one with an inner diameter of 0.96 mm, both displaying circular cross sections. Due to the huge difference between the channel diameters, two different experimental techniques and apparatuses have been employed. In both cases, during condensation tests, the heat is subtracted from the mixture by using cold water and the heat transfer coefficient is obtained from the measurement of the heat flux on the water side and the wall-to-refrigerant temperature difference. Both the test apparatuses are located at the Two-Phase Heat Transfer Lab of the University of Padova and even if they are different in size the schematic drawing is the same (Figure 1).

Each facility consists of a primary refrigerant loop and three auxiliary water loops. In the primary loop, the refrigerant exiting as subcooled liquid from the post-condenser is pumped by a magnetic driven gear pump through a Coriolis effect mass flow meter. Hence, the working fluid passes through an evaporator which consists of a tube-in-tube heat exchanger with hot water flowing on the external side. The superheated refrigerant is then sent to a pre-condenser to partially condense and to set the thermodynamic conditions.
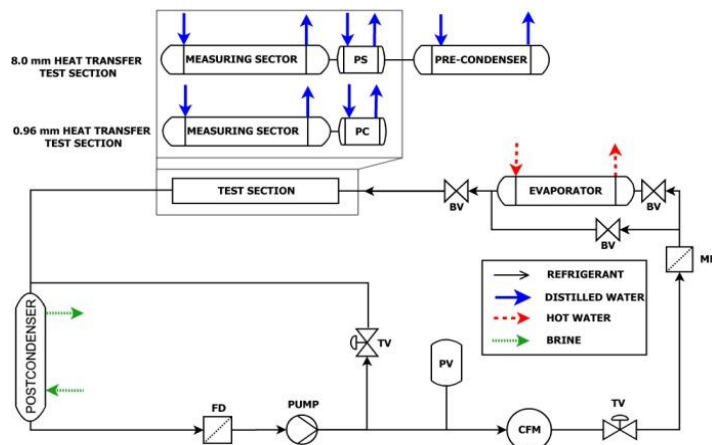
Figure 1 Experimental test rig: FD filter dryer; PV pressure vessel; CFM Coriolis-effect mass flow meter; TV valve; MF mechanical filter; BV ball valve; PS pre-conditioning sector; PC pre-condenser.
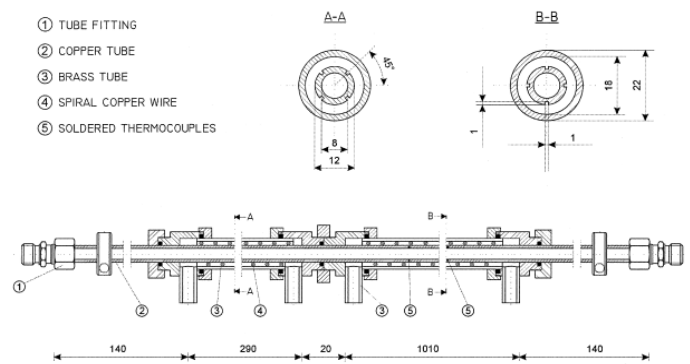
Figure 2 Technical drawing of the 8.0 mm test section.

In the 8.0 mm test section the pre-condenser is splitted in two parts: a tube-in-tube pre-condenser which is placed before the test section and a 300 mm pre-conditioning sector which is used to carefully check the vapor quality at the inlet of the actual measuring sector. In the two experimental test sections the fluid is condensed and the heat transfer coefficients are measured. After the test section the refrigerant is collected again in the post-condenser. On the cooling water side, in each circuit, the water temperature differences are measured using triple junction cooper-constantan thermopiles, the inlet water temperatures with copper-constantan thermocouples and the water mass flow rates using Coriolis mass flow meters and a magnetic type flow meter in the case of the pre-condenser of the 8.0 mm test section.

The 8.0 mm diameter heat transfer test section

This test section has an inner diameter of 8.0 mm and an internal longitudinal roughness *Ra* equal to 0.8 μm. It resembles a counter-current tube-in-tube heat exchanger, where the refrigerant condenses inside the smooth tube and the cooling water flows in the annulus. The test section is composed of two parts, a pre-conditioning sector and a measuring sector which are respectively 300 mm and around 1.0 m long. Refrigerant temperatures at inlet and outlet of the test section are measured using thermocouples inserted into the refrigerant flow. The absolute pressure at the inlet of the test section is measured with a digital strain gauge pressure transducer while the pressure difference over the test section is measured with a differential pressure transducer. Wall temperatures are measured with eight type-T copper-constantan thermocouples embedded in the tube wall; four thermocouples are placed 100 mm after the inlet of measuring section, and the other four are located 100 mm before the outlet. On each location, the four thermocouples are inserted and soldered into four equidistant axial grooves along the circumference of the tube (Figure 2). A complete description of the test section can be found in [4].

The 0.96 mm diameter heat transfer test section

This test section has an internal diameter of 0.96 mm, circular shape and inner surface roughness *Ra* equal to 1.3 μm. As the previous one it is composed of two parts: a 0.05 m long pre-condenser, which is used as desuperheater, and a 0.23 long measuring sector. Differently from the 8.0 mm diameter test section this one has been designed to measure local heat

transfer coefficients. The present experimental technique requires precise measurements of the water temperature profile which is in turn used for the determination of local heat fluxes (Figure 3). In the measuring sector, the local water temperature profile is determined from the readings of fifteen thermocouples placed in the water channel and the local wall temperatures are gauged by thirteen thermocouples embedded in the wall along the measuring sector. At the inlet of each sector, the pressure is gauged by means of two pressure transducers whereas a differential pressure transducer is employed to measure the pressure drop along the measuring sector. The refrigerant temperature at the inlet and outlet of each sector is measured with T-type thermocouples. In Matkovic et al. [5] a detailed description of the test section is reported.
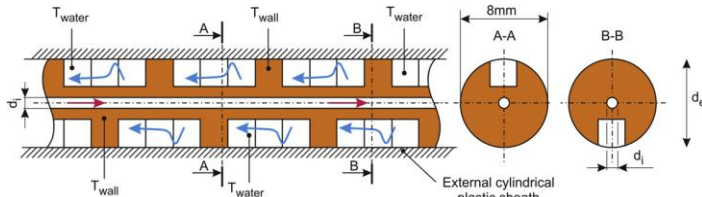
Figure 3 Sketch of the water coolant path in the 1 mm microchannel

MIXTURE COMPOSITION AND DATA REDUCTION

Condensation tests have been performed with the zeotropic mixture R455A, also named as L40X, which is a ternary mixture of R1234yf, R32 and CO_2 (75.5/21.5/3.0 by mass composition). In Table 1, some thermophysical and transport properties of the refrigerant blend are reported, compared with those of the main pure fluid components, R32 and R1234yf. Properties are computed using NIST Refprop 9.1 (Lemmon et al., [6]).

Table 1. Properties of mixture and pure components at 40°C saturation temperature.

Fluid	R32	R1234yf	R455A
GWP	675	4	145
p_{sat} [bar]	24,78	10,18	17,6
ρ_l [kg m^{-3}]	893,1	1033,8	989,1
ρ_g [kg m^{-3}]	73,3	57,7	80,5
ρ_l/ρ_g [-]	12,2	17,9	12,3
μ_l [μPa s]	95,0	128,8	112,0
λ_l [W m^{-1} K^{-1}]	0,115	0,059	0,073
T bubble [°C]	-	-	35,1
Glide [K]	-	-	9,81

Table 2 Refrigerant cycle data at mean temperatures 0/40 °C (5 K superheating, 3 K subcooling).

Fluid	R32	R1234yf	R455A	R404A	R410A
p_{evap} [bar]	8.13	3.16	5.5	6.05	6.7
p_{cond} [bar]	24.8	10.18	17.6	18.25	20.6
p_{cond}/p_{evap} [-]	3.05	3.22	3.20	3.02	3.07
Vol. cool. Cap [kJ m^{-3}]	5385	2020	3515	3450	4236
COP	5.42	5.47	5.39	5.18	5.40

In order to understand the impact on system performance and to check weaknesses and strengths of R455A, its theoretical cycle efficiency has been evaluated and compared to that of pure components and mixtures that will be phased down (R404A and R410A). A thermodynamic cycle composed of compressor, condenser, expansion device and evaporator has been examined. The evaporation and condensation processes are considered as isobaric and the compression isentropic, while superheating and subcooling have been fixed at 5 K and 3 K respectively. For pure fluids the evaporating temperature is set at 0°C and the condensing temperature at 40°C. For the zeotropic mixture, because of the temperature glide, condensing temperature has been computed as the mean of bubble and dew point temperatures, while the evaporating one has been chosen as the mean between evaporator inlet temperature and dew point temperature. Results from simulations are reported in Table 2 with evaporation and condensation pressures, pressure ratios, volumetric capacity and COPs. Mixture R455A has volumetric capacity comparable with those of R404A and R410A. Furthermore, R455A shows a COP value similar to that of R410A in the considered working conditions.

Data reduction

During a condensation test in the 8.0 mm smooth tube a mean heat transfer coefficient, along the measuring sector, can be obtained from Eq. (1):

$$\alpha = \frac{q_{MS}}{A_{MS}\,\Delta T_{LMTD}} \tag{1}$$

where q_{MS} is the heat flow rate exchanged over the measuring sector, A_{MS} is the exchange surface area of the measuring sector, and ΔT_{LMTD} is the logarithmic mean temperature difference between refrigerant and tube wall. In each i-sector, included the measuring one, the heat flow rate is obtained from an enthalpy balance on the cooling water side:

$$q_i = \dot{m}_{water,i}\,c_{p,water}\,\Delta T_{water,i} \tag{2}$$

where the water temperature difference between inlet and outlet is measured with triple junction cooper-constantan thermopiles and the water flow rate is measured with a Coriolis effect mass flow meter or, in the pre-condenser, with the magnetic-type flow meter.

The refrigerant enthalpy change in each i-sector is computed from the measured water side heat flux as follows:

$$\Delta h_i = \frac{q_i}{\dot{m}_{ref}} \tag{3}$$

considering that the enthalpy of the superheated vapor at the inlet of the pre-condenser can be determined from the measured pressure and temperature.

The inlet and outlet vapor qualities in each sector can be obtained from the local pressure p, enthalpy h and the overall composition of the mixture X_{mix} using Refprop 9.1, as:

$$x = f(p, h, X_{mix}) \tag{4}$$

The local pressure is computed assuming that the pressure changes linearly along the tube from the measured inlet and outlet pressure. The enthalpy at the inlet and the outlet of the measuring section are derived from energy balances, using Eqs. (2-3). Once the inlet and outlet vapor qualities have been calculated the mean quality can be derived and referred to the mean value of heat transfer coefficient.

Regarding the minichannel test section, the local heat flux can be determined from the slope of the water temperature profile (obtained from the thermocouples inserted along the coolant path):

$$q' = -\frac{\dot{m}_{water}\, c_{water}}{\pi\, d_i}\frac{dT_{water}(z)}{dz} \tag{5}$$

where z is the axial coordinate along the tube, dT_{water}/dz is the derivative of the polynomial equation interpolating the measured water temperature. The heat flow rate transferred to the secondary fluid at a certain position z is obtained integrating the local heat flux from the refrigerant inlet to the position z:

$$q(z) = \pi\, d_i \int_0^z q'(z)\, dz \tag{6}$$

The local heat transfer coefficient inside the minichannel is then obtained as:

$$\alpha(z) = \frac{q'(z)}{T_{ref}(z) - T_w(z)} \tag{7}$$

The wall temperatures T_w are measured with thermocouples embedded in the wall while the refrigerant temperature T_{ref} is calculated from the pressure p, the specific enthalpy h and the mixture composition in mass fraction X_{mix}:

$$T_{ref}(z) = f\left[p(z), h(z), X_{mix}\right] \tag{8}$$

Along the measuring sector, the local pressure is obtained starting from the measured inlet and outlet values and using models to better determine local and distributed contributions. The refrigerant enthalpy at a position z can be calculated as:

$$h(z) = h_{in,MS} - \frac{q(z)}{\dot{m}_{ref}} \tag{9}$$

During a condensation test run, the refrigerant mixture enters the pre-condenser as superheated vapour. In the pre-condenser the refrigerant is cooled down by the secondary fluid and the refrigerant enthalpy at the inlet of the measuring sector $h_{in,MS}$ is determined from a thermal balance on the water side. As for the refrigerant temperature, the vapor quality along the test section is evaluated using the local pressure, the local enthalpy and the mixture composition.

For condensation tests, the average experimental uncertainty of the heat transfer coefficient is 7% for the 8.0 mm diameter channel and 6% for the 0.96 mm microchannel.

CONDENSATION TESTS RESULTS

The experimental results obtained during the condensation of R455A in the 8 mm and 0.96 mm diameter channels are presented in Figs. 4 and 5. The condensation heat transfer coefficient are plotted versus local vapor qualities for three mass velocities G = 200-300-400 kg m^{-2} s^{-1}. For both the tested channels, the heat transfer coefficient is found to increase with mass velocity and to decrease when reducing the vapor quality. Comparing Figs. 4 and 5, it can be noticed that the heat transfer coefficient increases as the inner diameter of the tube

decreases. This influence of the tube diameter is usually predicted by correlations (i.e. during annular flow condensation Cavallini et al. [7] model, during single-phase heat transfer Dittus-Boelter equation) and the heat transfer coefficient is function of the tube diameter with a power law of -0.2. Considering the ratio between the diameters of the two channels, the heat transfer coefficients in the minichannel are expected to be 35% higher than those in the 8.0 mm diameter tube. From the experiments, the heat transfer coefficients inside the 0.96 mm diameter minichannel at G = 400 kg m^{-2} s^{-1} and G = 200 kg m^{-2} s^{-1} are higher respectively by 30-40% and by 13-23% than those in the 8.0 mm diameter tube, considering the whole vapor quality range. At G = 200 kg m^{-2} s^{-1} the difference between the performance in the two tubes is lower than expected. This can be related to the different flow patterns in the two channels: annular flow is expected to be the predominant in the 0.96 mm microchannel, while in the 8.0 mm tube stratified and stratified wavy flow are foreseen.
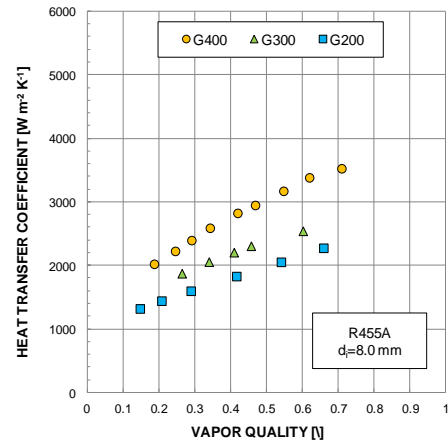
Figure 4 Experimental local heat transfer coefficient versus vapor quality for R455A (L40X) mixture measured in the 8.0 mm diameter channel (G is mass flux [kg m^{-2} s^{-1}]).
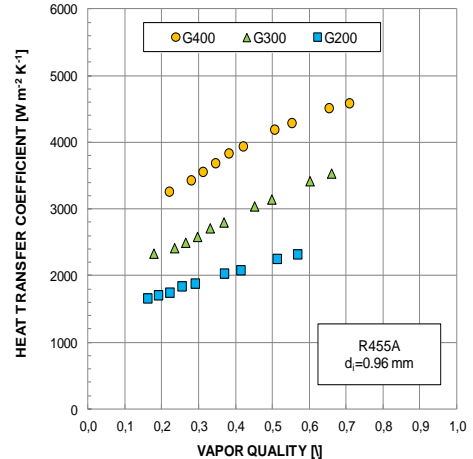
Figure 5 Experimental local heat transfer coefficient versus vapor quality for R455A (L40X) mixture measured in the 1 mm diameter minichannel (G is the mass flux [kg m^{-2} s^{-1}]).

The heat transfer mechanisms that occur during the condensation of zeotropic mixtures are the same as for pure fluids, convective condensation and film condensation during stratified flow, but they are affected by the zeotropic

characteristics of the blend. Actually, the condensation process results as non-isothermal with both liquid and vapor phase sensible heat effects. The sensible heat removal from the vapor is particularly significant because of the low heat transfer coefficients associated with this process. Furthermore, the diffusion resistances in both the vapor and the liquid phases are present due to the continuous change in the compositions of both phases, and between them the mass transfer resistance in the vapor phase is the most crucial aspect of this process. These mechanisms affect the condensation heat transfer process penalizing the performance of the mixture.

In Fig. 6 the heat transfer coefficients measured with R455A in the 1 mm diameter minichannel are plotted together with data taken in the same test section with R32 and R1234yf (data for pure components are reported in Matkovic et al. [5] and Del Col et al. [8]) at $G = 200$ kg m^{-2} s^{-1} and $G = 400$ kg m^{-2} s^{-1}. The highest heat transfer coefficients are obtained with R32: at $G = 400$ kg m^{-2} s^{-1} and $x = 0.3$ the heat transfer coefficient of R32 is 38% higher than those of R455A, and at $G = 400$ kg m^{-2} s^{-1} and $x = 0.6$ is nearly doubled. The heat transfer coefficients of R455A are similar to those of R1234yf. However, a complete comparison between different refrigerants during convective condensation should account not only for the heat transfer coefficient but also for the saturation temperature drop, which is not addressed here.

PREDICTION OF THE HEAT TRANSFER COEFFICIENT

When designing a heat exchanger working with zeotropic mixtures, the effect of the additional mass transfer resistance should be properly accounted for. Two methods widely used in the literature are those of Colburn and Drew [9] and Bell and Ghaly [10]: the first one adopts a more physically realistic treatment of the phenomenon, the second one is based on the equilibrium cooling curve and heat transfer considerations alone. The Bell and Ghaly [10] method, to account for the additional mass transfer resistance, is based on the assumption that complete mixing both in the liquid and in the vapor phase is reached and overall equilibrium is maintained. Bell and Ghaly [10] focused on the heat transfer problem because reasonable estimates of its resistance can be made from available information, and it is possible to bound the heat transfer problem in a conservative manner. Therefore, the key assumption in the Bell and Ghaly [10] procedure is that the effect of the mass transfer resistance in the vapor phase can be replaced by a conservative estimate of the heat transfer resistance in the vapor phase. Their assumptions lead to write the overall thermal resistance as sum of two thermal resistances in series:

$$\alpha_{mix} = \left(\frac{1}{\alpha_f} + \frac{\partial q_{sg}/\partial q_t}{\alpha_g} \right)^{-1} \tag{10}$$

where α_f is the condensate film heat transfer coefficient calculated with the model for pure fluids but using the thermophysical properties of the mixture, α_g is the convective heat transfer coefficient of the vapor phase flowing alone in the tube and calculated with the Dittus-Boelter equation, $\partial q_{sg}/\partial q_t$ is
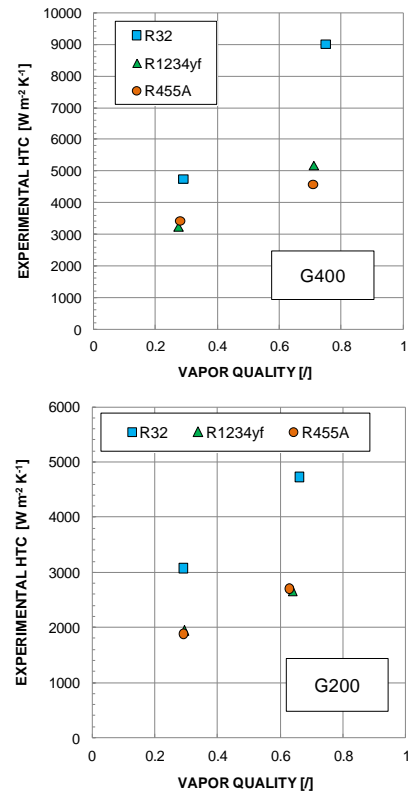
Figure 6 Heat transfer coefficients of R455A, R32 and R1234yf in 1 mm diameter minichannel at $G = 400$ kg m^{-2} s^{-1} (above) and $G = 200$ kg m^{-2} s^{-1} (below)

the ratio between sensible heat flow rate heating the vapor and total heat flow rate which can be expressed with good approximation as reported in Eq. (11).

$$\frac{\partial q_{sg}}{\partial q_t} \approx x c_{pg} \left(\frac{dT}{dh} \right) \tag{11}$$

If the ratio of dT/dh remains approximately constant during condensation, this ratio can be written as a function of the temperature glide and the enthalpy change of isobaric condensation:

$$\frac{dT}{dh} \approx \frac{\Delta T_{GL}}{\Delta h_{mix}} \tag{12}$$

The experimental heat transfer coefficient data taken in the 8.0 mm diameter channel have been compared with the predictions of Thome et al. [11] model for pure fluids corrected with the Bell and Ghaly [10] approach as suggested in Del Col et al. [12], Fig. 7. The model proposed by Thome et al. [11] is based on a flow patter map for condensation in horizontal plain tubes. The flow regimes classified in the map are: fully stratified, stratified-wavy, intermittent, annular and mist flow. The model slightly underestimates the heat transfer coefficient (mean absolute deviation $e_{AB} = 7.5\%$, standard deviation 3.9%).

In Del Col et al. [13] the Cavallini et al. [7] model corrected with the Bell and Ghaly [10] was applied to evaluate the condensation heat transfer coefficient of R32/R1234ze(E) mixtures in 1 mm microchannel. As reported in Matkovic et al. [5] and Del Col et al. [13], the Cavallini et al. model (2006),

which has been originally developed to predict the condensation heat transfer coefficient inside tubes with inner diameter greater than 3 mm, can be reasonably applied in the case of R32 and R1234yf to a 1 mm diameter minichannel if the mass velocity is higher or equal to 200 kg m^{-2} s^{-1}.

The comparison between experimental data and Del Col et al. model [13] is reported in Fig. 8. The model is able to predict the whole database within ±20%. The mean absolute deviation e_{AB} is less than 5% and the standard deviation is equal to 2.9%.
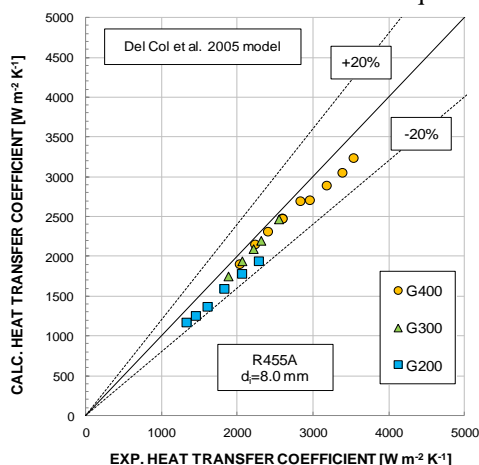
Figure 7 Experimental heat transfer coefficients of R455A (L40X) measured in the 8.0 mm diameter channel compared to values calculated with the Del Col et al. (2005) model.
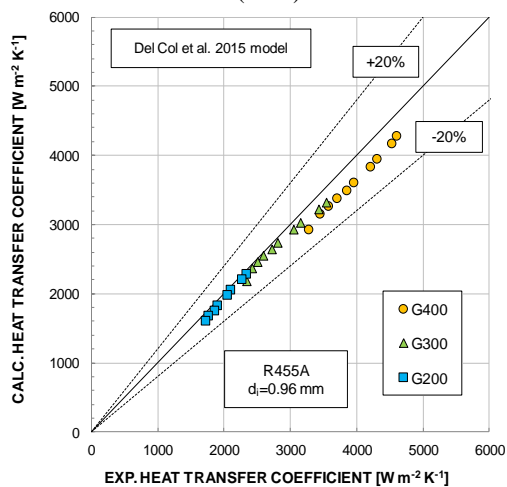
Figure 8 Experimental heat transfer coefficients of R455A (L40X) measured in the 1 mm diameter minichannel compared to values calculated with the Del Col et al. (2015) model.

CONCLUSIONS

This paper reports experimental heat transfer coefficients measured during condensation of low-GWP zeotropic blend L40X (ASHRAE designation R455A) inside a 8.0 mm and a 0.96 mm inner diameter horizontal smooth tubes. This zeotropic mixture displays a temperature glide of about 10 K. The experimental tests have been carried out at a mean saturation temperature of 40°C with mass velocities varying between 200 and 400 kg m^{-2} s^{-1}. The condensation heat transfer coefficient of R455A increases with vapour quality and mass velocity. Furthermore, due to the different diameter and, very likely, the flow pattern, they are higher in the 0.96 mm

diameter tube. With respect to pure components, heat transfer coefficients of R455A inside the 0.96 mm diameter minichannel are higher than those of R32 and comparable with those of R1234yf at the same operating conditions.

The new database has been compared with Del Col et al. [12] and with Del Col et al. [13] predicting models in the case of 8.0 mm inner diameter tube and 0.96 mm minichannel respectively. In both approaches, models for pure vapor condensation are corrected with the Bell and Ghaly [10] correlation to account for the additional mass transfer resistance. The models well predict the heat transfer coefficients with mean absolute deviations lower than 8%.

REFERENCES

[1] Hossain, M. A., Onaka, Y., Afroz, H. M. M., Miyara, A., Heat transfer during evaporation of R1234ze(E), R32, R410A and a mixture of R1234ze(E) and R32 inside a horizontal smooth tube, *Int. J. of Refrigeration,* Vol. 36, pp. 465-477, 2013.

[2] Kondou, C., Mishima, F., Koyama, S., Condensation and evaporation of R32/R1234ze(E) and R744/R32/R1234ze(E) flow in horizontal microfin tubes, *Science and Technology for the Built Environment,* 21, pp. 564-577, 2015.

[3] Wang, L., Dang, C., Hihara, E., Experimental and theoretical study on condensation heat transfer of non-azeotropic refrigerant mixture R1234yf/R32 inside a horizontal smooth tube, *Proceedings from International Refrigeration and Air Conditioning Conference at Purdue*, 2012.

[4] Cavallini, A., Censi, G., Del Col, D., Doretti, L., Longo, G. A., Rossetto, L., Experimental investigation on condensation heat transfer and pressure drop of new HFC refrigerants (R134a, R125, R32, R410A, R236ea) in a horizontal smooth tube, *Int. J. of Refrigeration,* 24, pp. 73-87, 2001.

[5] Matkovic, M., Cavallini, A., Del Col, D., Rossetto, L., Experimental study on condensation heat transfer inside a single circular minichannel, *Int. J. Heat Mass Transfer*, 52, pp. 2311-2323, 2009.

[6] Lemmon, E. W., Huber, M. L., McLinden, M. O., NIST Standard Reference Database 23: Reference Fluid Thermodynamic and Transport Properties-REFPROP, Version 9.1, National Institute of Standards and Technology, Gaithersburg, 2013.

[7] Cavallini, A., Censi, G., Del Col, D., Doretti, L., Matkovic, M., Rossetto, L., Zilio, C., Condensation in Horizontal Smooth Tubes: A New Heat Transfer Model for Heat Exchanger Design. *Heat Transfer Eng.*, 27(8), 31-38, 2006.

[8] Del Col, D., Torresin, D., Cavallini, A., Heat transfer and pressure drop during condensation of the low GWP refrigerant R1234yf, *Int. J. Refrig.*, 33, 1307-1318, 2010.

[9] Colburn, A. P., and Drew, T. B., The Condensation of Mixed Vapors, *Trans. AIChemE*, 33, pp. 197–215, 1937.

[10] Bell, K., Ghaly, M., An approximate generalized design method for multicomponent/partial condensers, *AIChE Symp. Ser*, 69, pp. 72-79, 1973.

[11] Thome, J. R., El-Hajal, J., Cavallini, A., Condensation in horizontal tubes, part 2: new heat transfer model based on flow regimes, *Int. J., Mass Transfer*, 46 (18), pp. 3365-3387, 2003.

[12] Del Col, D., Cavallini, A., Thome, J. R., Condensation of zeotropic mixtures in horizontal tubes: new simplified heat transfer model based on flow regimes, *J. Heat Transfer*, 127 (3), p. 221, 2005.

[13] Del Col, D., Azzolin, M., Bortolin, S., Zilio, C., Two-phase pressure drop and condensation heat transfer of R32/R1234ze(E) non-azeotropic mixtures inside a single microchannel, *Science and Technology for the Built Environment*, 21, pp. 595-606, 2015.